



Justyna Zygmuntowicz<sup>1\*</sup>, Paweł Falkowski<sup>2</sup>, Aleksandra Miazga<sup>1</sup>, Katarzyna Konopka<sup>1</sup>

<sup>1</sup>Warsaw University of Technology, Faculty of Materials Science and Engineering, ul. Wołoska 141, 02-507 Warsaw, Poland

<sup>2</sup>Warsaw University of Technology, Faculty of Chemistry, ul. Noakowskiego 3, 00-664 Warsaw, Poland

\*Corresponding author. E-mail: justyna.zygmuntowicz@inmat.pw.edu.pl

Received (Otrzymano) 05.07.2016

## ZrO<sub>2</sub>-Ni COMPOSITES - PROPERTIES AND CHARACTERIZATION

In recent years dynamic progress has been seen in almost all areas of engineering materials. It has contributed to the development of new, innovative materials such as composite materials. Nowadays, a great deal of research is focused on ceramic/metal composites due to their potential to be used in many applications. An example of such a material is ZrO<sub>2</sub>-Ni composites. This paper describes ZrO<sub>2</sub>-Ni composites formed by uniaxial pressing and sintering in an argon atmosphere. The microstructure, selected physical and mechanical properties such as hardness, fracture toughness and the biaxial strength of the composites were investigated. The sintered composites had a relative density close to 99% of the theoretical density. The distribution of the component phases was uniform. It was found that the presence of Ni particles affects the mechanical properties of the ZrO<sub>2</sub> matrix. It was also revealed that the composites exhibit a lower bending strength than ceramic materials obtained under the same conditions. The composites show a decrease in hardness in regard to the hardness of monolithic ZrO<sub>2</sub>. The presence of Ni particles in the composites causes dissipation of propagating crack energy, which results in an increased fracture toughness value measured for ZrO<sub>2</sub>-Ni composites in comparison to the value obtained for monolithic zirconia.

**Keywords:** composites ZrO<sub>2</sub>-Ni, uniaxial pressing, mechanical properties

## KOMPOZYTY ZrO<sub>2</sub>-Ni - WŁAŚCIWOŚCI I CHARAKTERYSTYKA

Dynamiczny postęp, jaki miał miejsce w ostatnich latach, widoczny jest praktycznie w każdym obszarze inżynierii materiałowej. Przyczynił się on do opracowania nowych materiałów, takich jak materiały kompozytowe. Obecnie, wiele badań dotyczy kompozytów ceramika/metal ze względu na ich duży potencjał aplikacyjny. Przykładem materiału z tej grupy jest kompozyt ZrO<sub>2</sub>-Ni. W artykule opisano kompozyty o podstawie tetragonalnego tlenku cyrkonu z dodatkiem niklu formowane na drodze prasowania jednoosiowego oraz spiekane w atmosferze argonu. W pracy opisano mikrostrukturę, wybrane właściwości fizyczne oraz właściwości mechaniczne, takie jak: twardość i odporność na kruche pękanie oraz wytrzymałość mechaniczną na zginanie otrzymanych spieków. Otrzymane spieki charakteryzowały się gęstością względną na poziomie 99% gęstości teoretycznej oraz jednorodnym rozmieszczeniem obu faz w mikrostrukturze kompozytu. W wyniku przeprowadzonych badań stwierdzono wpływ cząstek Ni na właściwości mechaniczne ZrO<sub>2</sub>. Stwierdzono, że kompozyty wykazują niższą wytrzymałość na zginanie niż materiały ceramiczne uzyskiwane w tych samych warunkach. Kompozyty wykazują spadek twardości w odniesieniu do twardości monolitycznego ZrO<sub>2</sub>. Obecność Ni w kompozytach prowadzi do rozpraszania energii pęknięcia, co powoduje wzrost wartości odporności na kruche pękanie kompozytów ZrO<sub>2</sub>-Ni w porównaniu do wartości uzyskanych dla monolitycznego ZrO<sub>2</sub>.

**Słowa kluczowe:** kompozyty ZrO<sub>2</sub>-Ni, prasowanie jednoosiowe, właściwości mechaniczne

## INTRODUCTION

Among various types of structural ceramics, zirconia ceramics have been widely researched in the recent years. This type of materials is characterized by thermal and chemical stability, high mechanical properties and biocompatibility, which allow its use for thermal coatings, cutting tools, biomedical implants etc. [1-7]. Nowadays many studies concern attaining improvement of the mechanical properties of ceramics. One of the methods is the introduction of a metallic phase into the ceramic matrix. The presence of metal particles can prohibit the propagation of cracks.

An interesting and attractive composite system may be the ZrO<sub>2</sub>-Ni composite material. This system may

cause expanded use of zirconia ceramics. ZrO<sub>2</sub>-Ni composites have good compatibility because of their similar thermal expansion coefficients and elastic modulus [8-10]. Moreover, the addition of nickel particles in the zirconia matrix can enhance both the strength and toughness of ceramics [11-13]. The advantage the ZrO<sub>2</sub>-Ni system is the fact that zirconia and nickel particles are readily available. The zirconia-nickel system thus has the potential to act as a model composite system, which is now widely studied by scientists [8-10, 14, 15]. However, the full characteristics of the microstructure and properties of this type of system are still lacking.

In the present study, nickel particles are added to a zirconia matrix. The physical and mechanical properties of the ZrO<sub>2</sub>-Ni materials were analyzed. The microstructure of the composites was also determined.

## MATERIALS AND METHODS

The starting materials were: ZrO<sub>2</sub> stabilized by 3 mol% Y<sub>2</sub>O<sub>3</sub> (TZ-3Y-SE) powder with 99.99% purity and an average particle size of 100 nm, and Ni powder (Alfa Aesar) with 99.99% purity and an average particle size of 150 μm. The particle sizes were measured by laser diffraction (Laser Particle Size Analyzer LA-960) conducted in a diluted well-dispersed suspension. The densities of ZrO<sub>2</sub> and Ni were 6.05 and 8.9 g/cm<sup>3</sup> respectively. The SEM observations revealed that the ZrO<sub>2</sub> powder is highly agglomerated. However, according to the results of the size measurements, it can be stated that they are weak agglomerates and during processing they can be partially broken (Fig. 1a). Figure 1b shows that the surface of the Ni particles is highly irregular with numerous cavities and the shape of the nickel particles resembles a cauliflower head.

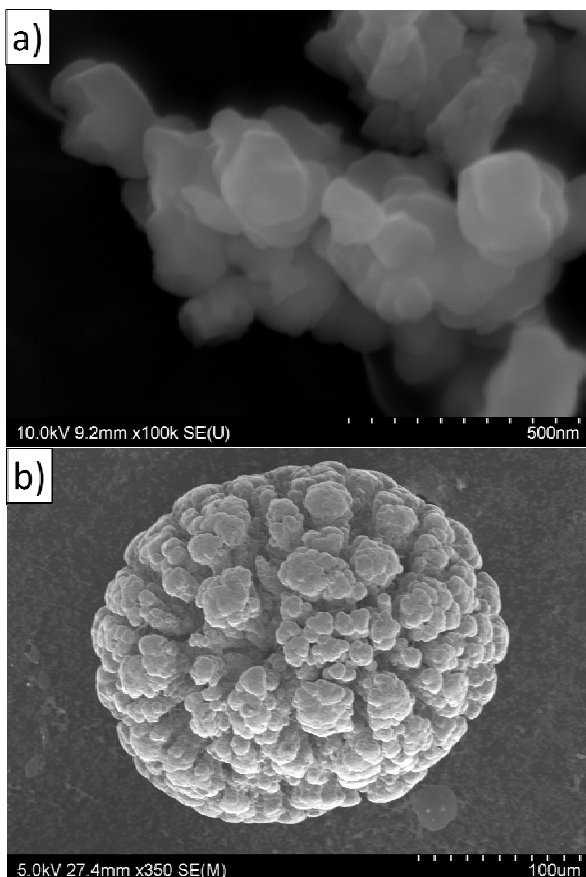


Fig. 1. Scanning electron micrograph of starting powders: a) ZrO<sub>2</sub> powder, b) Ni powder

Rys. 1. Wyjściowe proszki: a) proszek ZrO<sub>2</sub>, b) proszek Ni

The composites were prepared from the powder mixture containing: 90 vol.% ZrO<sub>2</sub> and 10 vol.% Ni powder. The composites were formed by uniaxial press-

ing at 100 MPa and sintering at 1600°C in an argon atmosphere. The scheme of ZrO<sub>2</sub>-Ni composite fabrication is shown in Figure 2.

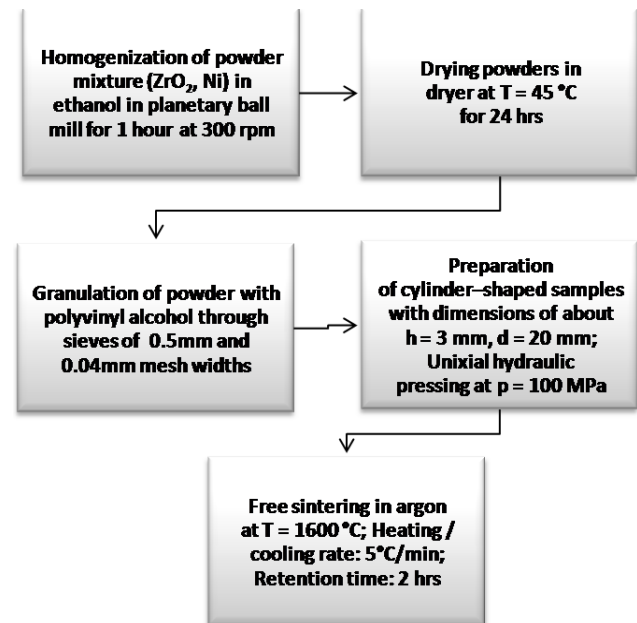


Fig. 2. Scheme of ZrO<sub>2</sub>-Ni composite preparation

Rys. 2. Schemat otrzymywania kompozytu ZrO<sub>2</sub>-Ni

XRD study was performed to determine the crystalline phases of the materials. It was conducted using a Rigaku MiniFlex II diffractometer with CuK<sub>α1.54</sub> ( $\lambda = 1.54178 \text{ \AA}$ ). The spectra were scanned at the rate of 1°/min in the range  $2\theta = 10\text{--}100^\circ$ . In order to measure the selected physical properties of the composites, the Archimedes method was used according to the PN-76/6-06307 standard. The theoretical density used to determine the relative density was calculated from the rule of mixtures equation. Observation of composite sample cross sections was performed using the optical microscope Nikon ECLIPSE LV150N and Scanning Electron Microscope HITACHI SU-70. Chemical analysis was conducted using a SEM with an EDS detector.

The bending strength of the composites was measured by the ball-on-ring (BOR) test [16-18]. The values were computed using Kirstein and Woole's equation:

$$\sigma_{max} = \frac{3P(1-\nu)}{4\pi t^2} \left[ 1 + 2\ln \frac{a}{b} + \frac{(1-\nu)}{(1+\nu)} \left\{ 1 - \frac{b^2}{2a^2} \right\} \frac{a^2}{R^2} \right] \quad (1)$$

where:  $P$  - the load [N],  $\nu$  - Poisson's ratio,  $t$  - disk thickness [m],  $a$  - radius of supporting ring [m],  $b$  - radius of ball (the region of uniform loading at the centre) [m],  $R$  - radius of sample [m].

For comparison, bending strength measurements for comparable homogeneous samples with monolithic zirconia were performed.

The hardness of the composites was measured by the Vickers method on a polished sample surface under a load of 10 kG (98 N) with a 10-second holding time. Based on measurements of the length of cracks propa-

gated from the corner of the hardness indentation, the fracture toughness of the material ( $K_{IC}$ ) was determined. In this study, a Vickers hardness indenter was applied to propagate what are called median cracks on the surface. The  $K_{IC}$  values in this case can be estimated using the equation [19]:

$$K_{IC} = 0.067 \cdot \left(\frac{E}{H_V}\right)^{0.4} \cdot \left(\frac{c}{a}\right)^{-1.5} \cdot H_V \cdot \sqrt{a} \quad (2)$$

where: E - Young's modulus,  $H_V$  - Vickers hardness, c - crack length [ $\mu\text{m}$ ], a - one half of the indent diagonal length [ $\mu\text{m}$ ].

## RESULT AND DISCUSSION

The XRD patterns of the composites after sintering at 1600°C show that the composites consist of two phases: ZrO<sub>2</sub> and Ni. The tetragonal zirconium dioxide (t-ZrO<sub>2</sub>) phase was observed because of stabilization of the ZrO<sub>2</sub> powder by 3 mol% yttrium oxide (Y<sub>2</sub>O<sub>3</sub>).

Figure 3 presents an example of the microstructure of the ZrO<sub>2</sub>-Ni composite sample. The nickel particles (white color) are homogeneously distributed throughout the ceramic matrix (grey) in the material. Despite the strongly irregular shape of the nickel particles during pressing and sintering, the ZrO<sub>2</sub> penetrated all the cavities and open pores. In such a way, it was possible to obtain a highly dense material with good connection between Ni and ZrO<sub>2</sub>. However, observation of the microstructure revealed the presence of small pores (black spots) throughout the volume of the material.

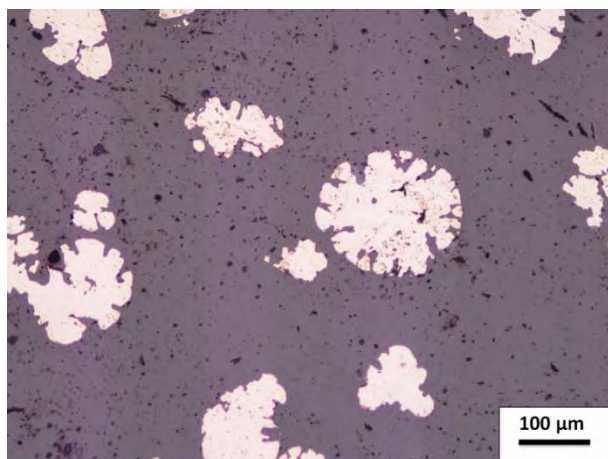


Fig. 3. Optical micrograph of ZrO<sub>2</sub>-Ni composite cross section  
Rys. 3. Mikrofotografia z mikroskopu optycznego kompozytu ZrO<sub>2</sub>-Ni

The measurement results of selected physical properties of the sintered samples are shown in Table 1. The green density was about 41.8% of the theoretical value. After the sintering process, the relative density was about 99.5%. Furthermore, the samples had an open porosity over 0.87%. The linear shrinkage of the sintered samples was 20.9% (measured at the height of the sample).

TABLE 1. Physical properties of sintered ZrO<sub>2</sub>-Ni composites measured by Archimedes method

TABELA 1. Właściwości fizyczne spieczonych kompozytów ZrO<sub>2</sub>-Ni obliczone na podstawie metody Archimede-  
desa

Physical properties		ZrO <sub>2</sub> + 10 vol.% Ni
Relative density	[%]	99.5 ± 0.46
Theoretical density	[g/cm <sup>3</sup> ]	6.33 ± 0.01
Apparent density	[g/cm <sup>3</sup> ]	6.30 ± 0.11
Open porosity	[%]	0.87 ± 0.94
Soaking	[%]	1.14 ± 0.15
Linear shrinkage	[%]	20.89 ± 0.81

Figure 4 shows the concentrations of nickel, zircon, yttrium and oxygen of ZrO<sub>2</sub>-Ni composite cross sections by using EDS investigation. The results of the concentration of nickel, zircon, yttrium and oxygen in a sample are collected in Table 2. From observations of the EDS measurements, it may be concluded that nickel particles were not oxidized to nickel oxide and there was no diffusion of nickel into the zirconia structure.

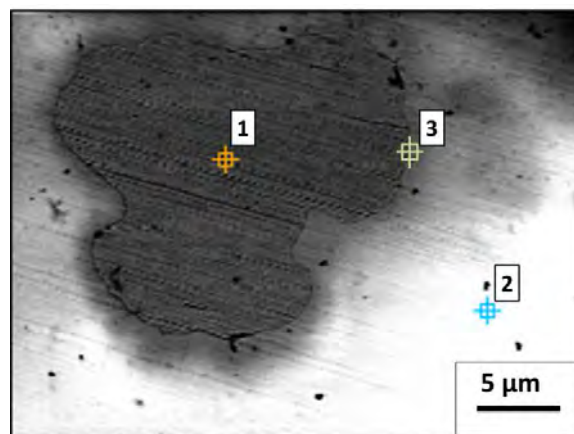


Fig. 4. EDS measurement of ZrO<sub>2</sub>-Ni sample with 10 vol.% metallic phase

Rys. 4. Analiza EDS składu chemicznego próbki ZrO<sub>2</sub>-Ni z 10% obj. zawartością fazy metalicznej

TABLE 2. Proportion by weight % and atomic % of elements of specimens measured in different areas

TABELA 2. Udział wagowy % i atomowy % poszczególnych pierwiastków w kompozycie

ZrO <sub>2</sub> -Ni composites				
Weight [%]				
	O	Ni	Y	Zr
area 1	0	100 ± 0.6	0	0
area 2	28.1 ± 0.4	0	6.8 ± 0.6	65.1 ± 0.7
area 3	20.0 ± 0.2	67.9 ± 0.4	0.5 ± 0.2	11.6 ± 0.3
Atom [%]				
	O	Ni	Y	Zr
area 1	0	100 ± 0.6	0	0
area 2	69.0 ± 0.9	0	3.0 ± 0.3	28.0 ± 0.3
area 3	49.2 ± 0.5	45.6 ± 0.3	0.2 ± 0.1	5.0 ± 0.1

The ball-on-ring test has been widely used to describe the biaxial strength of brittle materials [16-18]. The composite shows a lower bending strength than ceramic material obtained in the same conditions. In the case of the zirconia samples the values of bending strength amounted to  $705.73 \pm 71.75$  MPa, while in the case of the  $ZrO_2$ -Ni composites this value was  $574.08 \pm 44.25$  MPa. This difference may be due to the large particle size of the metallic phase in comparison to the matrix grains and the porosity of the composite sample.

The polished samples were used for Vickers hardness measurements. Figure 5 shows an example of the 98 N Vickers indentations in the  $ZrO_2$ -Ni composite. Due to the size and solids loading of the Ni particles, three kinds of indentation could be distinguished: full or partial indentation in an Ni particle, indentation close to Ni particles (in the range of cracks) and indentation in "pure"  $ZrO_2$ . That is why the obtained indentations in the  $ZrO_2$ -Ni composite were divided into these three groups and for each group the hardness was calculated. The average hardness for the composite also was calculated. The results of Vickers hardness of  $ZrO_2$  and the  $ZrO_2$ -Ni composite are shown in Table 3. The hardness of pure  $ZrO_2$  is similar to the hardness of monolithic

$ZrO_2$ . Due to the plasticity of the Ni particles, the hardness measured from the full or partial indentation in the Ni particle is much lower. The hardness calculated by indentation close to the Ni particles is between the hardness calculated for pure  $ZrO_2$  and direct indentation in the Ni particle. Generally, the addition of Ni particles decreases the hardness of zirconia.

Table 4 shows the values of fracture toughness determined by the indentation technique. In this case, the two different types of fracture toughness were calculated: fracture toughness after indentation in pure  $ZrO_2$  and fracture toughness after indentation close to Ni particles. Due to the lack of cracks, the fracture toughness based on direct indentation into Ni particles could not be calculated.

Similar to the hardness measurements, the fracture toughness of pure  $ZrO_2$  is similar to the hardness of monolithic  $ZrO_2$ . However, the fracture toughness calculated for the second case is about 35% higher than for pure  $ZrO_2$ . Hence, it could be stated that the addition of relatively big Ni particles into the zirconia matrix increases the fracture toughness of the composite. The average fracture toughness of  $ZrO_2$  and the  $ZrO_2$ -Ni composite is  $6.93$  and  $8.76$   $MPa \cdot m^{0.5}$  respectively.

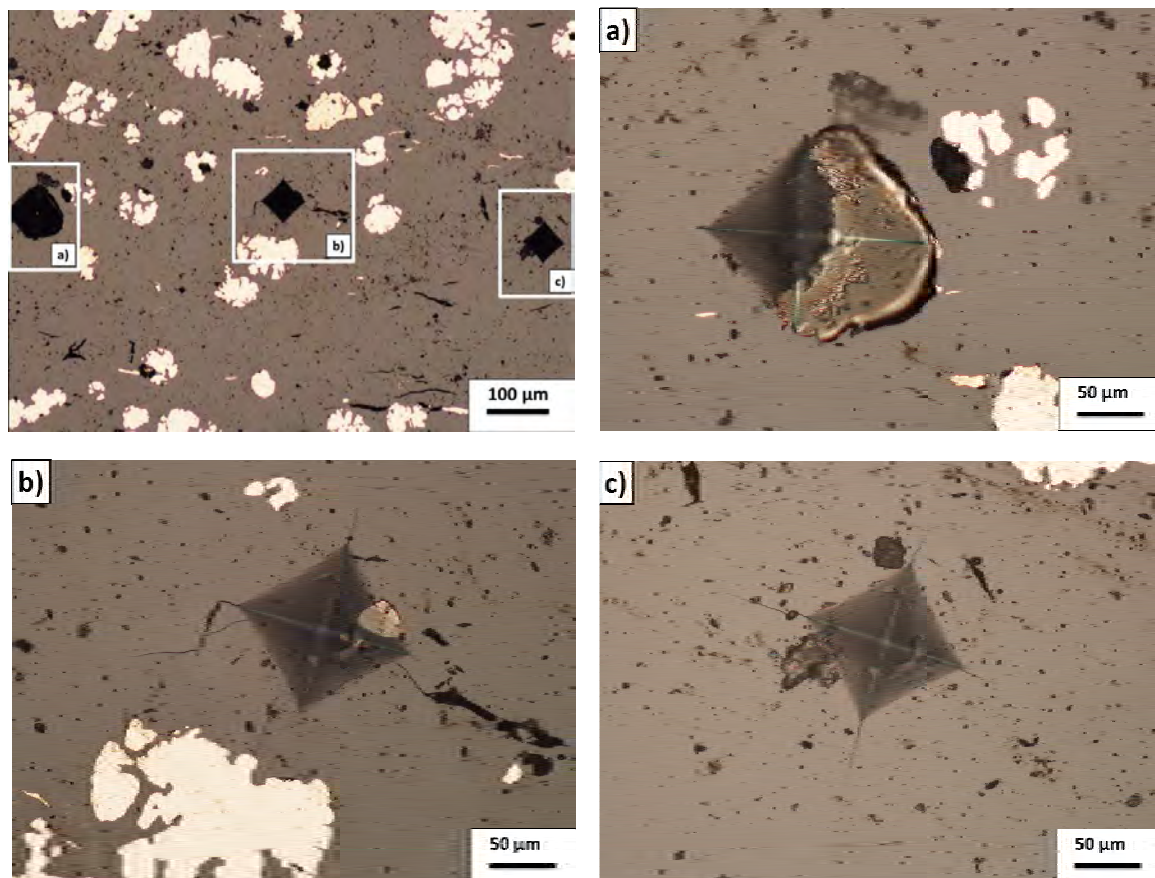


Fig. 5. Images from optical microscope of 98 N Vickers indentations in sintered  $ZrO_2$ -Ni composite: a) direct indentation in Ni particle, b) indentation near Ni particles, c) indentation in "pure"  $ZrO_2$

Rys. 5. Obrazy z mikroskopu optycznego odcisków Vickersa otrzymanych pod obciążeniem 98 N w spieczonej kształtce kompozytowej: a) odcisk piramidki bezpośrednio w cząstkę niklu, b) odcisk piramidki w pobliżu cząstki Ni, c) odcisk piramidki w „czystym”  $ZrO_2$

TABLE 3. Vickers hardness (HV<sub>10</sub>) after indentation in ZrO<sub>2</sub> and ZrO<sub>2</sub>-Ni composite  
 TABELA 3. Twardość Vickersa (HV<sub>10</sub>) dla ceramiki z ZrO<sub>2</sub> i kompozytu ZrO<sub>2</sub>-Ni

Material	Hardness HV <sub>10</sub> after indentation in "pure" ZrO <sub>2</sub> [GPa]	Hardness HV <sub>10</sub> after indentation close to Ni particles [GPa]	Hardness HV <sub>10</sub> after direct indentation in Ni particle [GPa]	Average hardness HV <sub>10</sub> [GPa]
ZrO <sub>2</sub>	11.20	---	---	11.20
ZrO <sub>2</sub> - 10 vol.% Ni	11.17	8.68	6.69	8.85

TABLE 4. Fracture toughness of ZrO<sub>2</sub> and ZrO<sub>2</sub>-Ni composite  
 TABELA 4. Odporność na kruche pęknięcie kształtek z ZrO<sub>2</sub> i kompozytu ZrO<sub>2</sub>-Ni

Material	Fracture toughness after indentation in pure ZrO <sub>2</sub> [MPa·m <sup>0.5</sup> ]	Fracture toughness after indentation close to Ni particles [MPa·m <sup>0.5</sup> ]	Average fracture toughness [MPa·m <sup>0.5</sup> ]
ZrO <sub>2</sub>	6.93	---	6.93
ZrO <sub>2</sub> - 10 vol.% Ni	6.95	10.58	8.76

## SUMMARY AND CONCLUSIONS

Using uniaxial pressing and the sintering process by applying the parameters of 100 MPa and 1600°C, enabled the formation of Ni-ZrO<sub>2</sub> composites. The sinters are characterized by a density of 6.3 g/cm<sup>3</sup>. The microstructure observation revealed homogeneous distribution of the Ni particles in the ZrO<sub>2</sub> matrix. It was found that the samples after sintering were characterized by two phases. The peaks of the tetragonal phase of zirconium dioxide stabilized by 3 mol% yttrium oxide and the peaks from nickel were identified. It was found that the composites show a lower bending strength than the ceramic materials obtained in the same conditions. The ZrO<sub>2</sub>-Ni composites show a decrease in hardness in regard to the hardness of the monolithic zirconia. The presence of nickel particles in the composites causes dissipation of propagating crack energy which results in increased fracture toughness value measured for ZrO<sub>2</sub>-Ni composites in comparison to the value obtained for monolithic zirconium.

## Acknowledgements

*This work was financially supported by the Faculty of Material Science and Engineering Warsaw University of Technology (statute work).*

## REFERENCES

- [1] Santos R.L.P., Buciumeanu M., Silva F.S., Souza J.C.M., Nascimento R.M., Motta F.V., Carvalho O., Henriques B., Tribological behaviour of glass-ceramics reinforced by Yttria stabilized zirconia, *Tribology International* 2016, 102, 361-370.
- [2] Stachowiak G.B., Stachowia G.W., Evans P., Wear and friction characteristics of ion-implanted zirconia ceramics, *Wear* 2000, 241, 220-227.
- [3] Fabris D., Souza J.C.M., Silva F.S., Fredel M., Mesquita-Guimarães J., Zhang Y., Henriques B., The bending stress distribution in bilayered and graded zirconia-based dental ceramics, *Ceramics International* 2016, 42, 11025-11031.
- [4] Kizaki T., Sugita N., Mitsuishi M., Experimental analysis of the machinability in the thermally assisted milling process of zirconia ceramics, *Precision Engineering* 2016, 45, 176-186.
- [5] Ajayan P.M., Schadler L.S., Braun P.V., *Nanocomposites Science and Technology*, Wiley-VCH Verlag, Weinheim 2003.
- [6] Manicone P.F., Iommetti P.R., Raffaelli L., An overview of zirconia ceramics: Basic properties and clinical applications, *Journal of Dental Research* 2007, 35, 819-826.
- [7] Gupta T.K., Bechtold J.H., Kuznicki R.C., Cadoff L.H., Rossing B.R., Stabilization of tetragonal phase in polycrystalline zirconia, *Journal of Materials Science* 1977, 12(12), 2421-6.
- [8] Tuan W.H., Liu S.M., Ho Ch.J., Biaxial strength of a ZrO<sub>2</sub>/(Ni+Al<sub>2</sub>O<sub>3</sub>) nanocomposite, *Journal of the American Ceramic Society* 2006, 89(2), 754-758.
- [9] Pecharroman C., Lopez-Esteban S., Bartolome J.F., Moya J.S., Evidence of nearest-neighbor ordering in wet-processed zirconia-nickel composites, *Journal of the American Ceramic Society* 2001, 84(10), 2439-2441.
- [10] Morales-Rodriguez A., Bravo-Leon A., Dominguez-Rodriguez A., Lopez-Esteban S., Moya J.S., Jimenez-Melendo M., High-temperature mechanical properties of zirconia/nickel composites, *Journal of the European Ceramic Society* 2003, 23, 2849-2856.
- [11] Taun W.H., Brook R.J., The toughening of alumina with nickel inclusions, *Journal of the European Ceramic Society* 1990, 6, 31-37.
- [12] Hannink R.H.J., Kelly P.M., Muddle B.C., Transformation toughening in zirconia-containing ceramics, *Journal of the American Ceramic Society* 2000, 83(3), 461-487.
- [13] Zhang D., Zhang L., Fu Z., Guo J., Tuan W.H., Differential sintering of Al<sub>2</sub>O<sub>3</sub>/ZrO<sub>2</sub>-Ni composite, during pulse electric current sintering, *Ceramics International* 2006, 32, 241-247.
- [14] Morales-Rodriguez A., Bravo-Leon A., Richter G., Ruhle M., Dominguez-Rodriguez A., Jimenez-Melendo M., Influence of oxidation on the high-temperature mechanical properties of zirconia/nickel cermets, *Scripta Materialia* 2006, 54, 2087-2090.
- [15] Moy J.S., Lopez-Esteban S., Pecharroman C., Bartolome J.F., Mechanically stable monoclinic zirconia-nickel composite,

- Journal of the American Ceramic Society 2002, 85(8), 2119-2121.
- [16] Shetty D.K., Rosenfield A.R., McGuire P., Bansal G.K., Duckworth W.H., Biaxial flexure tests for ceramics, American Ceramic Society Bulletin 1980, 59, 551-553.
- [17] Gijsbertus de With, Wagemans H.M., ball-on-ring test revisited, Journal of the American Ceramic Society 1989, 72, 1538-1541.
- [18] Chae S.H., Zhao J.H., Edwards D.R., Ho P.S., Verification of ball-on-ring test using finite element analysis, Thermal and Thermomechanical Phenomena in Electronic Systems 2016, 1-6.
- [19] Niihara K., A fracture mechanics analysis of indentation, Journal of Materials Science Letters 1983, 2, 221-223.